Analytical Methods

Deutsche Ausgabe: DOI: 10.1002/ange.201800455
Internationale Ausgabe: DOI: 10.1002/anie.201800455

Combinatorial Probes for High-Throughput Electrochemical Analysis of Circulating Nucleic Acids in Clinical Samples

*Jagotamoy Das, Ivaylo Ivanov, Tina S. Safaei, Edward H. Sargent, and Shana O. Kelley**

Abstract: *The analysis of circulating tumour nucleic acids (ctNAs) provides a minimally invasive way to assess the mutational spectrum of a tumour. However, effective and practical methods for analyzing this emerging class of markers are lacking. Analysis of ctNAs using a sensor-based approach has notable challenges, as it is vital to differentiate nucleic acids from normal cells from mutation-bearing sequences emerging from tumours. Moreover, many genes related to cancer have dozens of different mutations. Herein, we report an electrochemical approach that directly detects genes with mutations in patient serum by using combinatorial probes (CPs). The CPs enable detection of all of the mutant alleles derived from the same part of the gene. As a proof of concept, we analyze mutations of the EGFR gene, which has more than 40 clinically relevant alterations that include deletions, insertions, and point mutations. Our CP-based approach accurately detects mutant sequences directly in patient serum.*

Noninvasive analysis of circulating tumour-derived nucleic acids (ctNAs) is an appealing approach for cancer monitoring, as serial blood draws are possible for repetitive and longitudinal sampling, while solid tumours require invasive biopsies.[1] However, the reliable detection of nucleic acids containing mutations is very challenging as patient samples contain a very small percentage of mutated nucleic acids in a large background of normal nucleic acids.

Analysis of mutated nucleic acids in the blood, for example the *EGFR* (epidermal growth factor receptor) and *KRAS* (kirsten rat sarcoma viral oncogene homologue) genes, could allow specific monitoring of cancer-related sequences.[2] However, for detection of these mutated ctNAs, a very sensitive and specific method is required, as mutated ctNAs are present along with a high level of normal sequences. Currently, the most commonly used methods for ctNA analysis are DNA sequencing[3] and the polymerase chain reaction (PCR).[4] DNA sequencing is a powerful technique for research, but its application is restricted because of the high cost for routine clinical use and long turnaround time (2–3 weeks).[3d] Although conventional PCR methods cannot detect mutated ctNAs as they cannot detect minor variants at levels below 20%, some PCR-based methods, such as allele-specific clamp PCR, COLD-PCR (co-amplification at lower denaturation temperature-PCR), and digital PCR have successfully detected ctNAs.[4] However, PCR methods are susceptible to false negatives and positives produced by interference from chemical species present in clinical samples; the use of this approach therefore requires trained personnel and preprocessing of samples including purification of nucleic acids. This requirement limits the use of this technique to clinical laboratories. Thus, a PCR-free method that is able to detect mutated ctNAs directly in serum or blood is urgently needed to allow liquid biopsies for monitoring ctNAs to become more routine.

Chip-based electronic and electrochemical methods have been pursued as a promising alternative for clinical sample analysis because they can be automated and do not rely on costly instrumentation.[5] Particularly, electrochemical methods have received attention because of their low cost, high sensitivity, and amenability to high levels of multiplexing.[6] Electrochemical techniques have been employed successfully to analyze various tumour markers[7] and infectious pathogens,[8] but the analysis of ctNAs for tumour-related mutations in patient samples is a new application for this type of analysis that was first described less than three years ago.[9]

An electrochemical strategy developed by our laboratory for the analysis of a small set of point mutations in ctNAs was one of the first to address how a chip-based approach could facilitate ctNA analysis.[9] High-surface-area, three-dimensional microelectrodes were functionalized with probe sequences complementary to a sequence of interest, and hybridization of targets was read out with an electrocatalytic reporter strategy. PNA clamp molecules were used to limit cross-reactivity with wild-type nucleic acids and other mutated sequences. The technique specifically detected mutated ctNAs at physiologically relevant levels in 30–40 min. However, the *KRAS* and *BRAF* genes only contain point mutations in ctNAs. There many other sequence alterations that may appear in ctNAs. For example, *EGFR*, a sequence that is often mutated in lung cancer tumours, contains not only point mutations but also deletions and insertions.[10] However, analysis of *EGFR* is very challenging as it has more than 40 clinically relevant sequence changes.[10]

Herein, we report an electrochemical approach that enables the direct analysis of genes that have large panels of sequence alterations in ctNAs from patient serum (Figure 1). We designed combinatorial probes (CPs) that are able to screen all of the possible mutations present in the same region of the gene. For example, designing one CP enables the

[*] Dr. J. Das, Dr. I. Ivanov, Prof. S. O. Kelley
Department of Pharmaceutical Sciences
Leslie Dan Faculty of Pharmacy, University of Toronto
Toronto, ON M5S 3M2 (Canada)
E-mail: shana.kelley@utoronto.ca
Dr. T. S. Safaei, Prof. E. H. Sargent
Department of Electrical and Computer Engineering
Faculty of Engineering Department, University of Toronto
Toronto, ON (Canada)
Supporting information and the ORCID identification number(s) for the author(s) of this article can be found under: https://doi.org/10.1002/anie.201800455.

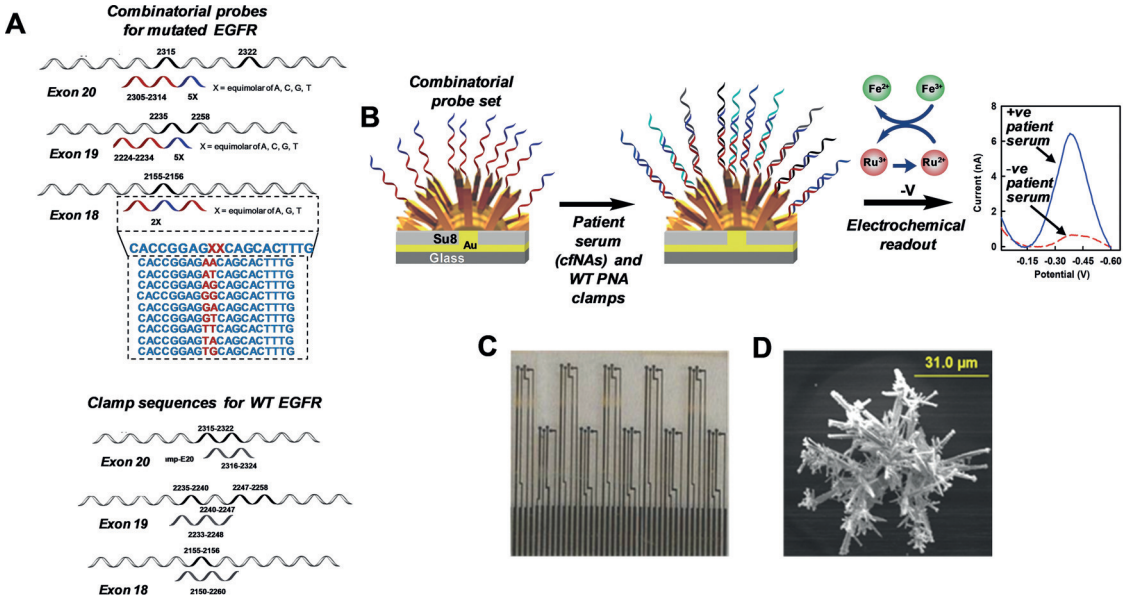

Figure 1. A) Top: Design of probes for the mutants of exons 18–20. X represents equimolar concentration of A, C, G, and T for CPs directed at exons 19 and 20, and an equimolar concentration of A, G, and T for the CP targeting exon 18. Numerical values, for example 2235 and 2258, correspond to the coding regions of the *EGFR* gene. Bottom: The CPs are used in conjunction with clamp sequences that bind to the wild-type target in solution and prevent it from binding to the sensor. B) NMEs formed on a multiplexed chips are functionalized with CPPs complementary to mutant target nucleic acids. Target ctNAs hybridize to the probes. Finally, after target-sequence binding and washing, the individual sensors were scanned in the presence of an electrocatalytic reporter system using differential pulse voltammetry. The DPVs shown were obtained with a sensor modified with CPP for deletion mutations at exon 19 before and after treating with NSCLC patient sample. C) Photograph of a multiplexed sensor chip. D) SEM image of an NME.

detection of all of the deletion mutations present at exon 19 (26 somatic mutations), another CP enables the detection of all of the insertion mutations at exon 20 (6 somatic mutations), and another CP enables the detection of all of the point mutations at exon 18 (3 somatic mutations). Designing 7 probes allows us to analyze all of the 40 somatic mutations of the *EGFR* gene directly in patient serum. The approach described allows the analysis of ctNA in patient samples with higher levels of throughput and mutational specificity than previously reported strategies.[9]

The design of the CPs for analysis of ctNA mutations is illustrated in Figure 1 A. We start with an analysis of *EGFR*. Mutations in *EGFR* genes are associated with a number of cancers, including lung cancer, anal cancers, and glioblastoma multiform; and the potency of targeted therapies are affected by mutations in this gene.[2] We design combinatorial PNA probes with variable positions in which X represents equimolar concentration of A, C, G, and T, at the N-terminal of the PNA probe (Figure 1 A). The combinatorial positions with the probes produce more favorable ΔG values for the complexes between CPs and mutated sequences than for the wild-type sequences and enables the CPs to bind mutant sequences specifically (see Supporting Information, Table 1). Moreover, to improve specificity further, PNA clamps are used to block the wild-type sequences in solution.[9]

Photolithography was used to produce an array of forty sensors for multiplexed ctNA analysis (Figure 1 C, see Supporting Information for all experimental details).[11] Gold contact pads and electrical leads were selectively patterned on the glass slides, which were pre-coated with chromium, gold, and a layer of positive photoresist. On top of this gold pattern, a layer of SU-8 was deposited and selectively developed to form an insulating top layer with 15 µm openings at the tips of the leads. Three-dimensional gold microsensors were then generated by electrodeposition of gold that produces anisotropic microneedles. Since nanostructuring enhances the sensitivity of the assay,[12] we electrodeposited the Au structures with a fine layer of Pd to produce nanostructured microelectrodes (NMEs). An SEM image of an NME is shown in Figure 1 D. These NMEs have been previously demonstrated to be effective in the specific detection of nucleic acids at subfemtomolar levels, even in the presence of complex biological fluids.[7a–d,8a–c,9]

We immobilized CPs specific to the mutant target of interest onto the sensors through a thiol linker (Figure 1 B). After target binding and washing, we used an electrocatalytic reporter system comprised of $[Ru(NH_3)_6]^{3+}$ and $[Fe(CN)_6]^{3-}$ to readout the presence of specific mutated nucleic acids sequences.[13] $[Ru(NH_3)_6]^{3+}$ is electrostatically attracted to the negatively charged phosphate backbone of nucleic acids that bind to the probes attached onto the surface of sensors and is reduced to $[Ru(NH_3)]_6^{2+}$ to generate an electrochemical signal when the electrode is biased at the reduction potential. This signal is highly amplified by adding $[Fe(CN)_6]^{3-}$, a more easily reduced anionic electron acceptor, which chemically oxidizes $[Ru(NH_3)_6]^{2+}$ back to $[Ru(NH_3)_6]^{3+}$ allowing for multiple turnovers of $[Ru(NH_3)_6]^{3+}$. This reporter system enables ultrasensitive detection of NAs without the need of enzymatic amplification. The change in current after target hybridization is used to determine target binding (typical

differential pulse voltammograms (DPVs) before and after application of the mutant positive patient serum are shown in Figure 1B).

To validate the approach, we first investigated whether CPs could identify different deletion mutations at exon 19. We individually challenged CP-functionalized NME sensors with different synthetic deletion mutant targets. For instance, we challenged CP-modified sensors with 4 deletion mutant targets individually (2235-2249 del15, 2235-2252 > AAT, 2236-2253 del18, and 2236-2250 del15). We also compared the current change when the same sensors were challenged with wild-type targets (E19DelWT). We observed that there was a clear positive current change for mutant targets (sensor 2 of Figure 2). After observing that the CP could detect deletion mutations, we investigated whether CP could also detect other mutations, such as insertion mutations at exon 20 (sensor 5) and point mutations at exon 18 (sensor 1). Sensor 5 was challenged with 3 insertion mutant targets (2319-2320 ins1, 2315-2316 ins2, and 2315-2316 ins3) and wild-type target (E20InsWT). Sensor 1 was challenged with 3 different point mutant targets at exon 18 (2155G > A, 2155G > T, 2156G > C) and wild-type target (2155-6 G). In addition, we tested the same sensor (sensor 1) with a solution containing a mixture of 3 point mutant targets (2155G > A, 2155G > T, and 2156G > C). For all of the cases, we observed a clear signal rise in the presence of at least one of the mutant targets. Moreover, as expected, the current change measured by sensor 1 for a mixed target solution was higher than that for individual targets. These results clearly suggest that CP can identify its targets successfully. We further validated other regular 4 PNA probes designed for other point mutations at different regions of *EGFR* (sensor 3, sensor 4, sensor 6, and sensor 7 of Figure 2).

To investigate the specificity of the approach, we challenged the sensor for insertion mutations (sensor 5) and the sensor for wild-type *EGFR* (sensor 8) with wild-type *EGFR* RNA isolated from A549 cell lines (Figure 3A). We observed

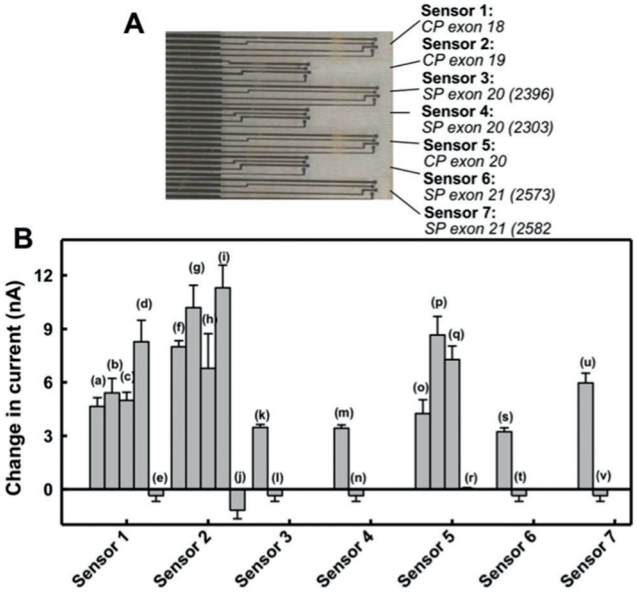

Figure 2. A) Multiplexed sensor strategy. Seven different types of sensors were generated by immobilizing sets of CPs or single probes (SPs) targeting different types of EGFR mutations on sensors arrayed on a multiplexed chip. B) Testing of sensors with synthetic targets. The *y*-axis indicates electrochemical current values obtained with different target/probe combinations. Sensor 1, exon 18 target sequences: a) 2155G > A mutant, b) 2155G > T mutant, c) 2156G > C mutant, d) mixed target solution containing (a–c), and e) wild-type; Sensor 2, exon 19 target sequences: f) 2235–2249 del15, g) 2235–2252 > AAT, h) 2236–2253 del18, i) 2236–2250 del15, and j) wild-type; Sensor 3, exon 20 target sequences: k) point mutant 2369C > T, and l) wild-type; Sensor 4, exon 20 target sequences: m) point mutant 2303G > T, and n) wild-type; Sensor 5, exon 20 target sequences: o) 2319–2320 ins1, p) 2315–2316 ins2, q) 2315–2316 ins3, and r) wild-type; Sensor 6, exon 21 targets: s) mutant 2573T > G and t) wild-type; Sensor 7, exon 21 targets: u) point mutant 2582A and v) wild-type. Concentration of target solution was 1 nM. All of the target solutions were mixed with 10 nM of clamps for wild-type.

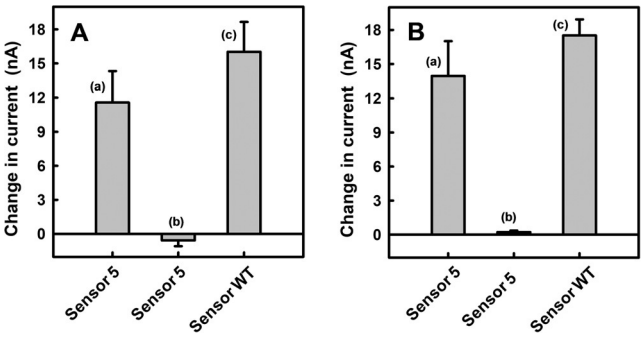

Figure 3. Sensors were modified with combinatorial probes for insertion mutations at exon 20 (Sensor 5) and wild-type probes (Sensor WT). A) The modified sensors were challenged with wild-type *EGFR* RNA (100 pg μL^{-1}) isolated from A549 cell lines in the presence (b) and absence (a,c) of PNA clamps for wild type. Combinatorial probes hybridize with wild-type *EGFR* RNA in absence of clamp. B) The modified sensors were challenged with ctNAs isolated from a healthy donor serum containing exon 20 fragments of *EGFR* before (a,c) and after (b) depletion with biotinylated oligonucleotides and streptavidin beads.

a signal increase for both of the sensors in absence of the clamps for the wild-type gene, highlighting the need for the clamp sequences to limit binding of the wild-type sequence. Next, to investigate the specificity of our sensor for *EGFR* genes versus other genes present in the human sample, we challenged sensor 5 (sensor for insertion mutations) and sensor 8 (sensor for wild-type) with samples of ctNA isolated from serum collected from a healthy donor with and without fragments of exon 20 of *EGFR* (exon 20 *EGFR* fragments were extracted from the latter sample using biotinylated oligonucleotides and streptavidin beads) (Figure 3B). No signal change was observed, for sensor 5 with exon E20 *EGFR*-depleted ctNAs, indicating that only *EGFR* can produce a significant signal on the sensors.

The final goal of our effort to develop a multiplexed mutation-discriminating chip is to enable the direct analysis of mutated sequences in patient samples. We elected to use samples from non-small cell lung cancer (NSCLC) patients for this validation study. As lung cancer samples could also contain *KRAS* mutations, a combinatorial probe was

Table 1: Multiplexed chips containing different *EGFR* sensors were challenged with eight NSCLC patient and two healthy donor serum samples.

Sample	G719X[a,b] (Sensor 1)	E19 Del[a,b] (Sensor 2)	T790M[a,b] (Sensor 3)	S768I[a,b] (Sensor 4)	E20 Ins[a,b] (Sensor 5)	L858R[a,b] (Sensor 6)	L861Q[a,b] (Sensor 7)	Results[c]
1	−0.3	1.0	−0.7	−0.7	0.3	−3.8	−1.6	E19 Del
2	−0.1	0.0	0.6	0.0	−0.3	−0.9	−1.3	T790M
3	1.5	0.0	−0.4	−0.4	7.6	−0.8	−0.4	G719X E20 Ins
4	−0.3	−0.3	−0.1	−0.5	−1.6	−0.6	−0.5	Wild type
5	−0.9	−1.4	−0.2	−1.1	−0.6	−0.3	−1.3	Wild type
6	2.6	−0.1	−0.7	0.0	0.0	0.0	−2.1	G719X
7	−0.8	4.2	−1.4	−2.1	−0.7	−1.5	−1.1	E19 Del
8	−1.1	2.5	−0.9	−1.3	−0.6	−1.0	−1.1	E19 Del
HD1	−1.7	−3.2	−2.0	−1.6	−0.3	−2.8	−0.2	Wild type
HD2	−0.9	−2.1	−0.1	−0.3	−0.5	−0.8	−1.6	Wild type

[a] Sensors 1–7 represent sensors of point mutants at exon 18, deletion mutants at exon 19, point mutant at exon 20 (c.2369C > T), another point mutant at exon 20 (c.2303G > T), insertion mutant at exon 20, point mutant at exon 21 (c.2573T > G), and another point mutant at exon 21 (c.2582T > A). [b] Negative current values reflect that post-incubation current levels were often lower than initial readings, likely reflecting changes in sensor surface functionalization after sample incubation. [c] The cut-off value for the sensors was 0.3 nA.

designed for mutated sequences and a conventional probe was generated for the wild-type sequence. These probes were immobilized on a multiplexed chip along with 8 probes for *EGFR* analysis. A wild-type *EGFR* sensor (sensor 8) was used as positive control and wild-type sensor for *KRAS* was used as negative control. We used our multiplexed chip to analyze ctNAs in serum samples from NSCLC patients (Table 1 and Supporting Information, Figure 1).

Six of the eight NSCLC patient samples were positive for *EGFR* mutations and four of the seven samples were positive for *KRAS* mutations. A threshold value for the CP assay was determined from the mean signal collected from a healthy donor serum plus three standard deviations. If the signal level collected with a patient serum was higher than the threshold value, the sample was considered to be mutant positive, and if it was lower, mutant negative. We also used a previously validated PCR method to confirm the presence or absence of the *EGFR* mutations in ctNAs isolated from same patient samples, and the results agreed with our approach (Tables 1 and 2).[11b]

It is noteworthy that in case of sample 3, the PCR assay identified only the E20 insertion mutation, whereas our CP assay also detected the E20 insertion mutation. In addition, our approach also identified a point mutation at exon 18 for the same sample. In the case of sample 6, although the PCR assay detected no mutation, our assay was successful in detecting a mutation in this sample. The CP assay thus successfully detects ctNA *EGFR* and *KRAS* mutations directly in the serum of NSCLC patients. We note that clamp PCR was not able to detect mutations directly in patient serum.[9a] Direct analysis of patient samples without purification, is a significant advantage as it eliminates any issues related to bias in the pool of sequences that are isolated.

In conclusion, we have analyzed ctNAs for a broad range of sequence alterations using a highly specific and sensitive electrochemical assay applicable to the analysis of serum samples of NSCLC patients. The approach can detect not only known mutations but also any unknown mutations in the same region of the genes. This assay could also detect any other genes in ctNAs with many somatic mutations or other sequences with significant mutational variation; for example, genotyping of drug resistant *Mycobacterium tuberculosis*. The use of a multiplexed chip in this strategy allows controls and self-calibration to be performed in parallel with the mutational analysis, increasing the reliability of the analysis. Minimally invasive, serum-based analysis of ctNA provides an alternative to tumour tissue biopsies and offers a new way for monitoring drug response and treatment efficacy. This approach allows for straightforward assay workflow, minimizes sample loss, and enables the analysis of small samples. The significantly reduced analysis time, which can be as short as thirty minutes, makes this approach more attractive compared to PCR or sequencing methods.

Acknowledgements

The research reported in this publication was supported by the Province of Ontario through the Ministry of Research, Innovation and Science (Grant #RE05-009), the Canadian Institutes of Health Research (Emerging Team Grant #RMF-111625), the Canadian Cancer Society Research Institute (Grant #70241), and the Natural Sciences and Engineering

Table 2: *EGFR* clamp PCR with total ctNAs isolated from lung cancer patient samples.

Sample[b]		G719X	E19 Del	T790M	S768I	E20 Ins	L858R	L861Q	Results[a]
1	ΔCt-1	0	3	−1	−1	−1	−4	−13	E19 Del
	ΔCt-2	12	9	13	13	13	16	25	
2	ΔCt-1	−1	0	3	−1	−5	−3	−3	T790M
	ΔCt-2	13	12	9	13	17	15	15	
3	ΔCt-1	1	−5	–	–	2.5	−5	–	E20 Ins
	ΔCt-2	9.5	15.5	–	–	8	15.5	–	
4	ΔCt-1	−2	−2.5	−2.5	−2	−3	−5	−4	Wild type
	ΔCt-2	12	12.5	12.5	12	13	15	14	
5	ΔCt-1	0	0	−2.5	−1	−3	−5	−5	Wild type
	ΔCt-2	11	11	13.5	12	14	16	16	
6	ΔCt-1	1	–	−2	−2	−4	−2	–	Wild type
	ΔCt-2	7	–	10	10	12	10	–	
7	ΔCt-1	0	4	0	–	−1	–	−5	E19 Del
	ΔCt-2	12	8	12	–	13	–	17	
8	ΔCt-1	−5	3	−3.5	–	−4	−5	−3	E19 Del
	ΔCt-2	14	6	12.5	–	13	14	12	
HD1	ΔCt-1	−3	–	−4	−5	−5	−5	−5	Wild type
	ΔCt-2	11.8	–	12.8	13.8	13.8	13.8	13.8	
HD2	ΔCt-1	0	0	−5	−5	−3	−1	−3	Wild type
	ΔCt-2	9.5	9.5	14.5	14.5	12.5	10.5	12.5	

[a] For the clamp PCR, $\Delta Ct\text{-}1 \geq 2$ was considered to be mutated and $\Delta Ct\text{-}1 < 0$ was considered to be non-mutated. If $0 < \Delta Ct\text{-}1 < 2$, another parameter, ΔCt-2, needed to be considered and $\Delta Ct\text{-}2 > 3$ is considered to be wild-type. [b] The cycle number in which a detectable signal is measured is referred to as the cycle threshold (Ct). ΔCt-1 values are calculated using the expression: ΔCt-1 = (Standard Ct) − (Sample Ct) and ΔCt-2 values are derived by analyzing Ct values of the non-PNA mix versus the Ct values of the samples, for example, ΔCt-2 = (Sample Ct) − (non-PNA mix Ct). The standard Ct is 35 for the 7500 AB thermocycler used for this experiment

Research Council of Canada (Grant #2016-06090). The opinions, results and conclusions are solely the responsibility of the authors and no endorsement by the funding agencies is intended or inferred.

Conflict of interest

The authors declare no conflict of interest.

Keywords: circulating tumour nucleic acids · EGFR · electrochemistry · KRAS · liquid biopsy

How to cite: *Angew. Chem. Int. Ed.* **2018**, *57*, 3711 – 3716
Angew. Chem. **2018**, *130*, 3773 – 3778

[1] a) E. Yong, *Nature* **2017**, *511*, 524 – 526; b) J. C. M. Wan, C. Massie, J. Garcia-Corbacho, F. Mouliere, J. D. Brenton, C. Caldas, S. Pacey, R. Baird, N. Rosenfeld, *Nat. Rev. Cancer* **2017**, *17*, 223 – 238; c) H. Schwarzenbach, D. S. B. Hoon, K. Pantel, *Nat. Rev. Cancer* **2013**, *11*, 426 – 437; d) D. C. García-Olmo, C. Domínguez, M. García-Arranz, P. Anker, M. Stroun, J. M. García-Verdugo, D. García-Olmo, *Cancer Res.* **2010**, *70*, 560 – 567; e) P. L. Bedard, A. R. Hansen, M. J. Ratain, L. L. Siu, *Nature* **2013**, *501*, 355 – 364; f) C. Bettegowda, et al., *Sci. Transl. Med.* **2014**, *6*, 224ra24; g) S. O. Kelley, *Acc. Chem. Res.* **2017**, *50*, 503 – 507.

[2] a) J. Kaiser, *Science* **2010**, *327*, 1072 – 1074; b) A. Winther-Larsen, C. Demuth, J. Fledelius, A. T. Madsen, K. Hjorthaug, P. Meldgaard, B. S. Sorensen, *Br. J. Cancer* **2017**, *117*, 704 – 709; c) S. Xu, F. Lou, Y. Wu, D.-Q. Sun, J.-B. Zhang, W. Chen, H. Ye, J.-H. Liu, S. Wei, M.-Y. Zhao, et al., *Cancer Lett.* **2016**, *370*, 324 – 331; d) A. R. Thierry, F. Mouliere, S. El Messaoudi, C. Mollevi, E. Lopez-Crapez, F. Rolet, B. Gillet, C. Gongora, P. Dechelotte, B. Robert, et al., *Nat. Med.* **2014**, *20*, 430 – 435.

[3] a) F. Diehl, et al., *Nat. Med.* **2008**, *14*, 985 – 990; b) A. M. Newman, S. V. Bratman, J. To, J. F. Wynne, N. C. W. Eclov, L. A. Modlin, C. L. Liu, J. W. Neal, H. A. Wakelee, R. E. Merritt, et al., *Nat. Med.* **2014**, *20*, 548 – 554; c) J. Shendure, S. Balasubramanian, G. M. Church, W. Gilbert, J. Rogers, J. A. Schloss, R. H. Waterston, *Nature* **2017**, *550*, 345 – 353; d) F. E. Dewey, S. Pan, M. T. Wheeler, S. R. Quake, E. A. Ashley, *Circulation* **2012**, *125*, 931 – 944.

[4] a) J. Li, L. Wang, H. Mamon, M. H. Kulke, R. Berbeco, G. M. Makrigiorgos, *Nat. Med.* **2008**, *14*, 579 – 584; b) R. Lehmann-Werman, et al., *Proc. Natl. Acad. Sci. USA* **2016**, *113*, E1826 – E1834; c) Z. Zuo, S. S. Chen, P. K. Chandra, J. M. Galbincea, M. Soape, S. Doan, B. A. Barkoh, H. Koeppen, L. J. Medeiros, R. Luthra, *Mod. Pathol.* **2009**, *22*, 1023 – 1031; d) K. S. Thress, et al., *Nat. Med.* **2015**, *21*, 560 – 562; e) M. Baker, *Nat. Methods* **2012**, *9*, 541 – 544; f) X. Wang, et al., *Am. J. Gastroenterol.* **2011**, *106*, 2104 – 2111.

[5] a) S. O. Kelley, C. A. Mirkin, D. R. Walt, R. F. Ismagilov, M. Toner, E. H. Sargent, *Nat. Nanotechnol.* **2014**, *9*, 969 – 980; b) A. Gao, N. Lu, Y. Wang, P. Dai, T. Li, X. Gao, Y. Wang, C. Fan, *Nano Lett.* **2012**, *12*, 5262 – 5268.

[6] a) A. T. Sage, J. D. Besant, B. Lam, E. H. Sargent, S. O. Kelley, *Acc. Chem. Res.* **2014**, *47*, 2417 – 2425; b) M. Labib, E. H. Sargent, S. O. Kelley, *Chem. Rev.* **2016**, *116*, 9001 – 9090; c) A. Furst, S. Landefeld, M. G. Hill, J. K. Barton, *J. Am. Chem. Soc.* **2013**, *135*, 19099 – 19102; d) J. D. Besant, J. Das, I. B. Burgess, W. Liu, E. H. Sargent, S. O. Kelley, *Nat. Commun.* **2015**, *6*, 6978.

[7] a) J. Das, K. B. Cederquist, A. A. Zaragoza, P. E. Lee, E. H. Sargent, S. O. Kelley, *Nat. Chem.* **2012**, *4*, 642 – 648; b) J. Das, M. A. Aziz, H. Yang, *J. Am. Chem. Soc.* **2006**, *128*, 16022 – 16023; c) J. D. Besant, J. Das, I. B. Burgess, W. Liu, E. H. Sargent, S. O. Kelley, *Nat. Commun.* **2015**, *6*, 6978; d) J. Das, S. O. Kelley, *Anal. Chem.* **2011**, *83*, 1167 – 1172; e) E. Bakker, Y. Qin, *Anal. Chem.* **2006**, *78*, 3965 – 3983; f) K. Chuah, L. M. H. Lai, I. Y. Goon, S. G.

Parker, R. Amal, J. J. Gooding, *Chem. Commun.* **2012**, *48*, 3503 – 3505; g) S. S. Mahshid, S. Camire, F. Ricci, A. Vallee-Belisle, *J. Am. Chem. Soc.* **2015**, *137*, 15596 – 15599; h) H. Yang, A. Hui, G. Pampalakis, L. Soleymani, F.-F. Liu, E. H. Sargent, S. O. Kelley, *Angew. Chem. Int. Ed.* **2009**, *48*, 8461 – 8464; *Angew. Chem.* **2009**, *121*, 8613 – 8616; i) Y. Wan, Y.-G. Zhou, M. Poudineh, T. S. Safaei, R. M. Mohamadi, E. H. Sargent, S. O. Kelley, *Angew. Chem. Int. Ed.* **2014**, *53*, 13145 – 13149; *Angew. Chem.* **2014**, *126*, 13361 – 13365; j) E. Vasilyeva, B. Lam, Z. Fang, M. D. Minden, E. H. Sargent, S. O. Kelley, *Angew. Chem. Int. Ed.* **2011**, *50*, 4137 – 4141; *Angew. Chem.* **2011**, *123*, 4223 – 4227; k) Y. Wu, R. Y. Lai, *Chem. Commun.* **2013**, *49*, 3422 – 3424; l) M. A. McWilliams, R. Bhui, D. W. Taylor, J. D. Slinker, *J. Am. Chem. Soc.* **2015**, *137*, 11150 – 11155.

[8] a) J. Das, S. O. Kelley, *Anal. Chem.* **2013**, *85*, 7333 – 7338; b) J. D. Besant, J. Das, E. H. Sargent, S. O. Kelley, *ACS Nano* **2013**, *7*, 8183 – 8189; c) B. Lam, J. Das, R. D. Holmes, L. Live, A. Sage, E. H. Sargent, S. O. Kelley, *Nat. Commun.* **2013**, *4*, 1 – 8; d) K. Hsieh, A. S. Patterson, B. S. Ferguson, K. W. Plaxco, H. T. Soh, *Angew. Chem. Int. Ed.* **2012**, *51*, 4896 – 4900; *Angew. Chem.* **2012**, *124*, 4980 – 4984; e) B. S. Ferguson, S. F. Buchsbaum, T.-T. Wu, K. Hsieh, Y. Xiao, R. Sun, H. T. Soh, *J. Am. Chem. Soc.* **2011**, *133*, 9129 – 9135.

[9] a) J. Das, I. Ivanov, L. Montermini, J. Rak, E. H. Sargent, S. O. Kelley, *Nat. Chem.* **2015**, *7*, 569 – 575; b) J. Das, I. Ivanov, E. H. Sargent, S. O. Kelley, *J. Am. Chem. Soc.* **2016**, *138*, 11009 – 11016.

[10] S. V. Sharma, D. W. Bell, J. Settleman, D. A. Haber, *Nat. Rev. Cancer* **2007**, *7*, 169 – 181.

[11] B. Lam, R. D. Holmes, J. Das, M. Poudineh, A. Sage, E. H. Sargent, S. O. Kelley, *Lab Chip* **2013**, *13*, 2569 – 2575.

[12] a) L. Soleymani, Z. Fang, E. H. Sargent, S. O. Kelley, *Nat. Nanotechnol.* **2009**, *4*, 844 – 848; b) X. Bin, E. H. Sargent, S. O. Kelley, *Anal. Chem.* **2010**, *82*, 5928 – 5931; c) P. De Luna, S. S. Mahshid, J. Das, B. Luan, E. H. Sargent, S. O. Kelley, R. Zhou, *Nano Lett.* **2017**, *17*, 1289 – 1295.

[13] M. A. Lapierre, M. M. O'Keefe, B. J. Taft, S. O. Kelley, *Anal. Chem.* **2003**, *75*, 6327 – 6333.

Manuscript received: January 11, 2018
Revised manuscript received: January 30, 2018
Accepted manuscript online: February 1, 2018
Version of record online: March 2, 2018

